Electrochimica Acta 130 (2014) 771–777

Contents lists available at ScienceDirect

Electrochimica Acta

journal homepage: www.elsevier.com/locate/electacta

Low cost, simple three dimensional electrochemical paper-based analytical device for determination of p-nitrophenol

Murilo Santhiago [a,b,1,2], Charles S. Henry [c], Lauro T. Kubota [a,b,*,1,2]

[a] Department of Analytical Chemistry, Institute of Chemistry–UNICAMP, P.O.Box 6154, Campinas, Brazil
[b] National Institute of Science and Technology in Bioanalytics, Institute of Chemistry–UNICAMP, P.O.Box 6154, Campinas, Brazil
[c] Department of Chemistry, Colorado State University, Fort Collins, CO 80523, USA

ARTICLE INFO

Article history:
Received 16 January 2014
Received in revised form 26 February 2014
Accepted 22 March 2014
Available online 31 March 2014

Keywords:
Paper-based analytical devices
Pencil
p-nitrophenol
Electrochemical detection
Point-of-need.

ABSTRACT

We report here the fabrication and electrochemical characterization of a three-dimensional paper-based analytical device made from pencil (hard and soft) and paper as a low-cost, simple, easy-to-use device for p-nitrophenol analysis. The three-dimensional device integrates filtration and was fabricated from conventional printing paper patterned with a wax printer. A quick response code (QR) was added to the device to enable the user to rapidly assess p-nitrophenol information. The counter electrode was drawn on the paper while the working electrode consisted of a short section of graphite obtained from a pencil (30 × 0.3 mm). p-Nitrophenol was selected as the target analyte and basic parameters such as solution pH, buffer concentration, and pulse amplitude were optimized. Under optimized conditions (0.1 M acetate buffer, pH 4.0), a detection limit of 1.1 μM was obtained. The devices showed high sensitivity and a linear range for p-nitrophenol, 10 to 200 μM. The devices were employed to determine p-nitrophenol in water samples and the results showed recoveries ranging from 91.8 to 108.2%.

1. Introduction

The use of insecticides and pesticides in agricultural has increased dramatically over the past several decades [1]. Many of these molecules are extremely toxic to humans and are associated with numerous health problems [1,2]. In addition, insectides can undergo biodegradation process to form harmful byproducts [2]. p-Nitrophenol (pNP) is one example that can be found in wastewater and agricultural run-off due to biodegradation of parathion and methyl parathion [3]. The harmful effects of pNP on humans varies depending on exposure time and includes headaches, fever, breathing trouble and even death at high levels of exposure [4]. As a result, monitoring pNP in water is important, and many analytical techniques have been described to detect this molecule [5–8]. There is also a need for simple, disposable, point-of-need, low-cost and fast analysis systems for toxic pollutants to provide cost effective exposure risk assessment [9,10].

In recent years there has been a renewed interested in disposable analytical devices that are easy-to-use, low cost, and can be used at the point-of-need [11]. The device substrate is one important consideration for minimizing cost while achieving portability [9,11]. Paper has been used to construct paper-based analytical devices (μPADs) because of its broad availability, low cost, ease modification and simple manipulation [9,11,12]. μPADs can be fabricated using a variety of methods [13–16]. Among the fabrication methods, wax-printing is the most common and has been successfully used to create devices with colorimetric, chemiluminescent and electrochemical detection [13,16].

Electrochemical detection for paper-based analytical devices (ePADs) is attractive because it uses small, inexpensive instrumentation and can achieve low detection limits with high sensitivity [17,18]. To date, many electrode materials including gold [19,20] silver [21] and carbon [22] have been used in paper-based platforms. The low cost, easy fabrication, wide potential window and inert nature of carbon make it an attractive material for electrode fabrication [23–26].

Graphite pencils are an attractive electrode material for paper-based analytical devices. Pencils are cheap, available in many different diameters and lengths, found in every part in the world and are highly conductive [27]. The carbon content in pencils is specified by two main grades, which can be H (less carbon) and B (more carbon) [27]. As a consequence, B grade pencils have higher

* Corresponding author. Tel.: +55 019 3521 3127; fax: +55 918 3521 3023.
E-mail addresses: chuck.henry@colostate.edu (C.S. Henry), kubota@iqm.unicamp.br (L.T. Kubota).
[1] Tel.: +55 19 3521 3127.
[2] Tel.: +55 19 3521 3127.

http://dx.doi.org/10.1016/j.electacta.2014.03.109
0013-4686/

graphite to clay ratios making easier to leave a black trace on paper. Following this line, Bontempelli' group demonstrated the construction of carbon electrodes by directly drawing conductive tracks using a grade B pencil [28,29]. However, in order to achieve better electrochemical characteristics H grade pencils are the best choice due to lower background currents, lowest ΔEp and peak-to-peak current ratios close to one [30]. On the other hand, it is difficult to fabricate conductive tracks on paper using harder pencils, which turns necessary the construction of a new layout to couple the working electrode while keeping the main advantages of paper-based devices.

Here the fabrication of a three-dimensional electrochemical paper-based device using either graphite H or 6B is reported with the goal of providing better electrochemical responses along with a simple, easy-to-use and low-cost ePAD for the determination of p-nitrophenol.

2. Experimental

2.1. Materials and Equipment

All chemicals were of analytical grade and used as received. Conventional printing paper was acquired from a local bookstore. Whatman #1 chromatography paper was acquired from Merck (São Paulo, Brazil). p-Nitrophenol (pNP) was acquired from Merck (Darmstadt, DE). Potassium ferricyanide, potassium ferrocyanide, phenol, 4-aminophenol and 1,4 dihydroxy benzene were acquired from Sigma-Aldrich (St. Louis, MO). Sodium hydroxide, disodium phosphate (Na_2HPO_4) and monosodium phosphate (NaH_2PO_4) were acquired from Synth (SP, Brazil). Potassium chloride was obtained from J. T. Baker (NJ, USA). Acetic acid was from TEDIA (Fairfield, USA) and sodium acetate from Merck (Rio de Janeiro, Brazil) and were also used as received. The reagents were weighed on an analytical balance (Sartorius model BP 211D Goettingen, Germany) to 5 decimal places. A XEROX ColorQube 8570 printer from XEROX (Campinas, Brazil) was used to print the devices.

A hot plate from Fisatom was used to melt the wax. Pencil graphite H (0.3 mm x 60 mm) from Pentel and pencil graphite 6B from General' were used for electrode fabrication. Araldite® epoxy resin from Brascola (SC, Brazil) was used for sealing the pencil leads. Double- and single-sided tapes were purchased from a local bookstore.

The solutions were prepared using purified water in a MilliQ Millipore system (Billerica, MA, USA) and a Corning pH/Ion Analyser model 350 (Corning, NY, USA) was used to measure the solution pH. Working standard solutions were prepared daily by dilution of the stock solutions with 0.1 M Acetate buffer at pH 4.0.

2.2. Fabrication of the electrodes

The counter electrode was fabricated using a 6B pencil to fill the designated area. The graphite was applied for 1.5 minutes to provide electrical contact. The morphology of the paper surface before and after drawing was imaged using a JEOL JSM-5610LV scanning electron microscope (SEM).

The fabrication procedure for the working electrode is described below. Briefly, pencil graphite was cut and sealed using glass capillary tubes and epoxy resin. Before the electrochemical experiments, the electrodes were polished with alumina (0.3 μm) and washed with water to remove weakly adsorbed alumina particles [31]. After fabrication, pencil graphite electrodes (PGEs) were attached to paper using double-sided tape.

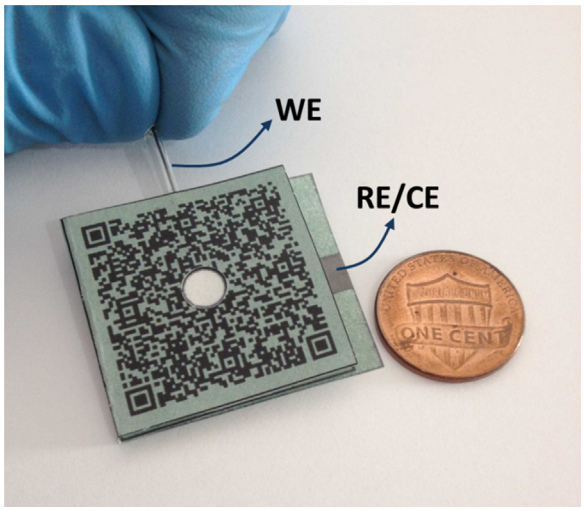

Fig. 1. Picture of the QR code with an integrated two-electrode system.

2.3. Construction of the Electrochemical Paper-based Devices (ePADs)

For the construction of the ePADs, designs were printed on conventional printing paper A4 size (210 × 297 mm) using a solid ink printer (ColorQube 8570). The printed paper was heated on a hot plate at 115 °C for 120s. After this process, the thermally treated paper was allowed to cool to room temperature and the QR (Quick response) code printed on top of the wax using the same printer. QR codes are a two-dimensional code that hold additional information in an easy to read format by most smartphones [32].

We initially printed an entire sheet of paper with a selected color. We have selected the contrast of green to black to fabricate our devices Fig. 1. The QR codes were constructed using free software (http://www.qrstuff.com). The information to be read was typed in the space provided for the code construction. After generation, the code has been copied and positioned on one of the device faces. After heating, the QR code, folding line and RE/CE line were printed on paper surface (Fig. 2, step (a)). The QR code was designed to have 625 mm^2 with a distance to the edges of 2 mm. After that, the face of the device containing the RE/CE line was treated in a hot plate (Fig. 2b). *Caution: The face of the QR code cannot touch the hot plate or the information will be lost. Fold the device and use a forcep to touch only RE/CE face.* Next, the paper was flipped and double-sided tape was inserted. On the other face, a pencil was used to make the reference electrode (Fig. 2, step(c)). Biopsy punches of 4 and 6 mm were used to open small circles on the center of the double-sided tape and QR code faces, respectively (Fig. 2, step (d)). For step (e), a hydrophobic black square of 15 × 15 mm with a hydrophilic circle (d = 5 mm) was created using Whatman #1 chromatography paper and attached on the backside of the QR code using single-sided tape, taking care to not cover the hydrophilic circle. The pencil graphite was attached on the paper-based device using double-sided tape, as shown in Fig. 2f. To prevent the sample pH from affecting response, a drop of the buffer was adding during the filtration layer preparation and allowed to dry before use.

2.4. Electrochemical Measurements and QR Code Reading

For the electrochemical measurements, the PGE was positioned horizontally as shown in Fig. 2f. For the analysis, 100 μL of sample or standard was added to the filtration zone created in the center of the QR code. Alligator clamps were used to make electrical contact to the electrodes on the ePAD.

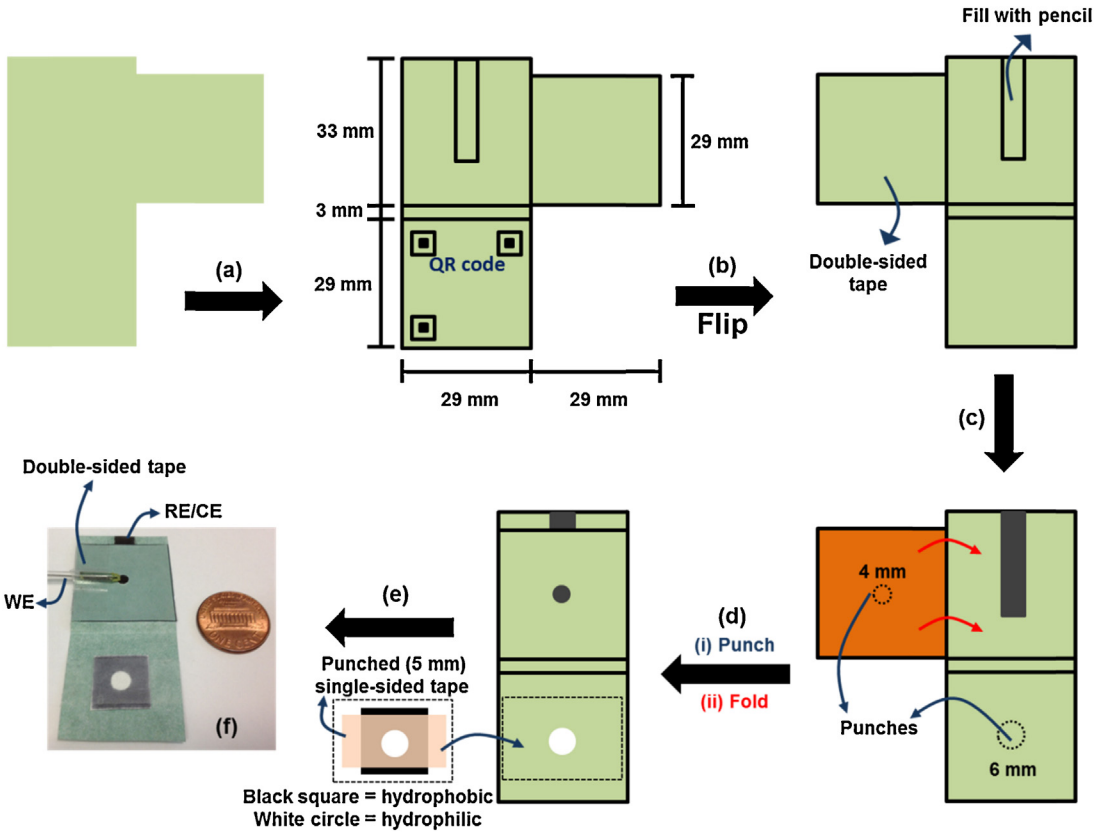

Fig. 2. Construction steps for the ePQR. (a) Printed QR code and alignment lines. (b) Heat treatment of the face designed for the construction of the RE/CE system (face 33 × 29 mm). (c) Drawn RE/CE and inserted double-sided tape. (d) The devices were punched and folded. (e) A punched single-sided tape was used to attach a black hydrophobic square (225 mm^2) containing a hydrophilic circle (d = 5 mm) on the opposite face of the QR code. (f) Picture of the attached WE on the device.

The voltammetry experiments were carried out with a PGSTAT-12 potentiostat/galvanostat from Autolab Eco Chemie (Utrecht, The Netherlands) connected to a PC (Software GPES 4.9). For the electrochemical experiments, a two-electrode system was employed using a single carbon counter-electrode (CE) and a PGE working electrode (WE). The differential pulse voltammograms were obtained at 50 mV s^{-1} in the potential range of 0.0 to 1.2 V *versus* carbon.

Tap water from three locations was collected and analyzed for p-nitrophenol. The samples were fortified with 40 μM of pNP and analyzed as described above. The instructions and more information on pNP detection were accessed using an iPhone model 4S (Apple) using a QR code reader.

3. Results and Discussion

3.1. Device Layout

A two-electrode system was selected to facilitate the measurement procedure and the coupling with the QR code because of the fabrication and operational simplicity of this configuration. For ePAD fabrication, we used conventional printing paper because it is readily available, lower cost than filter paper, and no flow is required through the device. The QR code size was 25 × 25 mm with a 2 mm quiet zone, defined as the distance between the code and the edges (Fig. 2) to make it easier for the QR code reader [32]. A filtration spot was created in the center of the QR code and aligned with the RE/CE system using a folding step. Double-sided tape was used to attach the WE to the top device layer. The horizontally attached pencil was positioned close to the reference electrode to minimize IR drop. In our case, the three-dimensional format (2D code with filtration spot + pencil graphite) is important because it makes electrode (both WE and CE/RE) and filter spot alignment easier. In this format, the filtration process is easily performed, the analyst only needs to add the sample and wait.

3.2. SEM images of the paper-based platform

The paper-based platform morphology was characterized before and after graphite deposition using scanning electron microscopy. Fig. 3(a) shows scanning electron micrographs of the wax-patterned paper after the heat treatment. The image shows a fibrous structure where the pores in the paper are filled by wax and other reagents. Printing paper are typically modified with chemicals or additives to improve surface properties [33]. After the electrode fabrication procedure, a significant change in the paper morphology is observed with the paper fibers being covered with graphite sheets (Fig. 3(b)). Fig. SD 1 shows more images at different magnifications. The carbon film had no cracks and wrinkles demonstrating the viability of the simple and low cost procedure to create conductive and flexible tracks on paper-based platforms.

3.3. Electrochemical Characterization

The first experiments were conducted using two and three electrode systems in order to compare the response of the graphite CE/RE with a traditional reference electrode. From Fig. 4a it can be observed that regardless of whether the experiments are on paper or in a conventional electrochemical cell, the current response is essentially the same as confirmed by running a statistical test (t-student) using anodic peak currents from the voltammograms. A negative peak shift of 203 mV was observed, as expected,

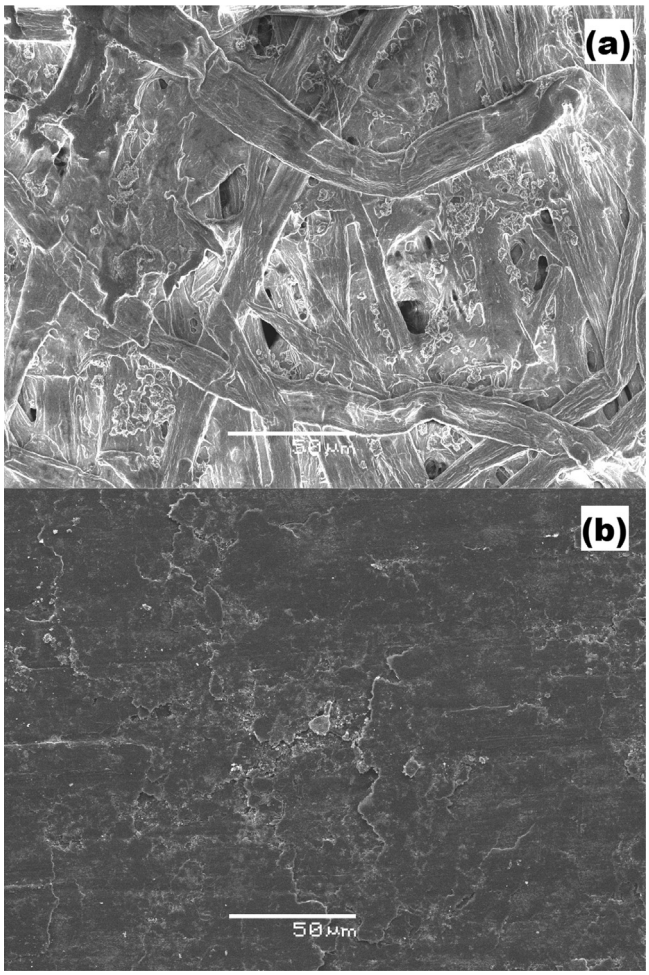

Fig. 3. Scanning electron micrographs of the paper before (a) and after (b) the pencil drawing procedure.

shifting the formal potential (Epa + Epc/2) to 0 V *versus* C. The reason for the cathodic shift is expected because the reference and working electrodes are made from the same material and dipped in the same solution [34]. The PGE gives a normalized peak-to-peak current ratio of ~1.0 and peak-to-peak separation (ΔEp) of 96 mV. The separation of anodic and cathodic peaks is higher than expected for ideal reversible electrochemical processes (ΔEp ~ 60 mV for one electron) [35], but is lower than reported for some screen-printed electrodes [36]. These results demonstrate the viability of the approach for making accurate and sensitive measurements.

The electrochemical oxidation of 200 μM pNP at the ePAD is shown in Fig. 4b. The cyclic voltammogram for the first cycle shows a well-defined oxidation peak at 0.9 V vs. carbon in the forward scan and no peak in the reverse scan. As the electrode is cycled, the peak current associated at the oxidation process decreases and the peak potential shifts toward more positive potentials. This result suggests that the products of the electrochemical reaction of pNP are adsorbing on the PGE surface, as previously described [37]. As a result of this electrode fouling, first run results are reported for all subsequent experiments. The influence of the scan rate was also studied. Fig. 4c shows the cyclic voltammograms for scan rates of 10–50 mV s^{-1}. As can be observed, the current associated with the electrochemical oxidation process increases as the scan rate increases as expected. The anodic peak currents were plotted against square root of the scan rate and a linear correlation was found (Fig. 4d), indicating that the electroactive species reaches the electrode by diffusion [35]. Also, the anodic peak potential does not shift toward more positive potentials indicating facile electrode kinetics.

Since the ePAD code is disposable, one of the main concerns is that the approach should have low relative standard deviations. We prepared and tested 8 devices and found a relative standard deviation of 6.3% by measuring pNP levels of 200 μM. The deviation is acceptable considering the construction process is manual.

3.4. Effect of pH and Supporting Electrolyte Concentration

The effect of solution pH from 2.5 to 8.0 on the ePAD response was evaluated by measuring the peak current in the cyclic voltammograms. As can be observed in Fig. 5a, the electrochemical response for pNP oxidation decreased as the solution pH increased. Graphite pencils are usually fabricated using kaolinite, solvents and graphite powder [38]. Kaolinite is a clay mineral which has negative charges in its structure and may be repelling negative charged molecules like pNP on higher pH values. Thus, the higher electrochemical responses were found when pNP solution was prepared in the pH range of 2.5 - 4.5 (pKa = 7.16) [39].

The impact of buffer concentration was evaluated next. Typically, conventional electrochemical experiments are done using electrolyte concentrations at least 100 times higher than the analyte [40]. Fig. 5b shows the influence of the supporting electrolyte concentration on the response of the device. As can be observed, the response reaches a plateau at 25 mM and remains constant for higher concentrations. Basically, the small size of the PGE minimizes ohmic drop effects (IR drop) making it possible to obtain voltammograms even at low supporting electrolyte concentrations. In the absence of supporting electrolyte, the ePAD still gives > 80% of the maximum response, however, the anodic peak shifts toward more positive potentials (SD 2).

3.5. Differential Pulse Voltammetry (DPV)

Differential pulse voltammetry was selected for the analytical application of the ePAD to water samples. DPV is among the most sensitive electrochemical techniques. In order to improve the detection limit of pNP, the impact of pulse amplitude was first optimized. Amplitudes from 10 to 200 mV were investigated (SD 3). The anodic peak current increased from 10 to 125 mV and then remained constant until 200 mV. Thus, 125 mV was selected for the remaining experiments.

The analytical curve for pNP determination was constructed using the ePAD using the conditions of higher response obtained so far. Fig. 6a shows the DPVs obtained for different pNP concentrations. The peak potential variation observed in Fig. 6a can be attributed to the triboelectric effect, which is a type of contact electrification, due to mechanical drawing process [41]. The analytical curve was linear from 10 to 200 μM (Fig. 6b) and can be described by the following equation:

$$Ipa(nA) = 30.2(\pm 3.6) + 7.6(\pm 0.1)\ [\text{p-nitrophenol}](\mu M) \quad (1)$$

with a correlation coefficient of 0.998. The limit of detection (LOD) was found to be 1.1 μM and calculated as being the concentration which produced a signal-to-noise (S/N) ratio of 3.

The maximum concentration of pNP to protect freshwater and saltwater aquatic life should not exceed 4.0 μM and 0.86 μM [42], respectively. The United States Environmental Protection Agency (EPA) has set the concentration of this class of compound at 72 μM to protect human health [43]. The ePAD has a LOD lower than the values above reported, except for the analysis of saltwater aquatic life samples where it is higher but still comparable.

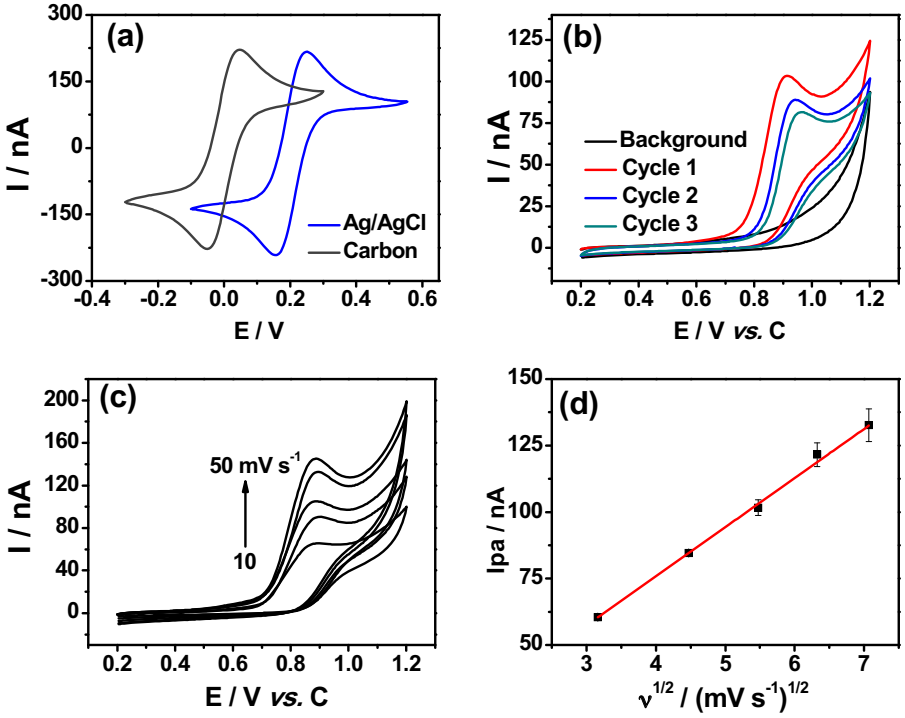

Fig. 4. (a) Cyclic voltammograms recorded in 0.1 M KCl solution containing 1 mM $Fe(CN)_6^{4-/3-}$ at 30 mV s^{-1} using a three electrode system (blue line) and ePQR with two electrodes (grey line). (b) Cyclic voltammograms obtained at 30 mV s^{-1} in the absence (background) and presence of 200 μM pNP in 0.1 acetate buffer solution at pH 4.0. (c) Cyclic voltammograms obtained for different scan rates 10–50 mV s^{-1} in the presence of 200 μM pNP in 0.1 acetate buffer solution at pH 4.0. (d) Plot of anodic peak current *vs.* square root of the scan rate. The error bars indicate the standard deviation of three devices.

3.6. Filtration System for ePADs

Water samples may present dispersed solid particles, one of the first steps adopted in laboratories of analysis is the filtration. To combine the filtration system with the QR code a piece of chromatographic paper was incorporated to the device. The size of the circle in the QR code is the only factor that can hinder the decodification process. We have observed that for circles up to 6 mm in diameter there is no reading complication. Thus, the contribution of the hydrophilic circle diameter on the collected volume was studied. Fig. 6c shows a graph of the collected volume (back face) versus filtration time. The procedure adopted to measure the volume in the back face is described in SD 4. As can be observed, the collected volume increases as function of time for a fixed diameter. To obtain fast response devices, the filtration time can also be reduced by increasing the diameter of the filtration spot. Here, a filtration zone of 5 mm and 40 s for the filtration time (volume ~ 25 μL) were selected for further experiments. One point that should be highlighted is the sample volume that is applied on the spot for filtration. The volume of the sample is not need to have a strict control, being one drop enough.

3.7. Study of interferences

For studying potential interferences, compounds with a similar chemical structure and same functional group were selected. Thus, VPDs were obtained in the presence of 4-aminophenol, 1,4 dihydroxy benzene and phenol using the optimized conditions. No interference in the peak current for pNP was observed when all compounds ([interferents and pNP] = 50 μM) were tested in 0.1 M acetate buffer at pH 4.0 (Fig. SD 5).

3.8. Water Sample Analysis

We selected tap water samples from three locations, spiked them with pNP and used the ePAD to measure the levels of pNP for the selected samples. We have included information in the QR

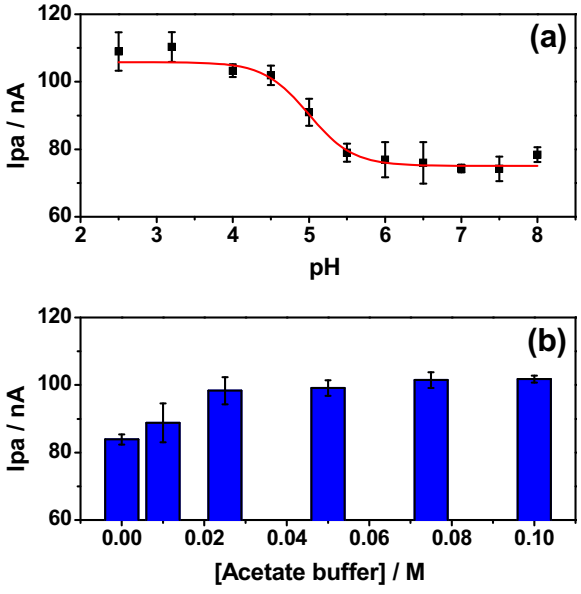

Fig. 5. (a) Graph of anodic peak current versus solution pH for 0.1 M buffers. (b) Anodic peak current *vs.* acetate buffer concentration. Conditions: The voltammograms were obtained in the presence of 200 μM pNP at 30 mV s^{-1}. The error bars indicate the standard deviation of three devices.

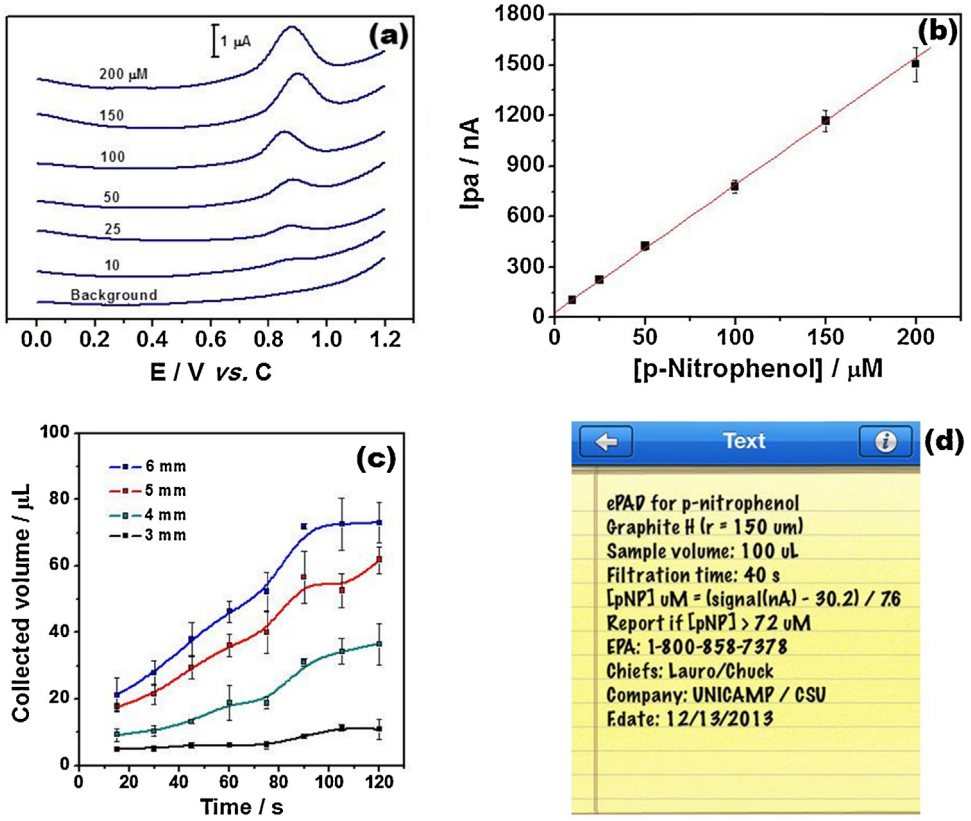

Fig. 6. (a) Differential pulse voltammograms (DPVs) obtained for different concentrations of pNP in 0.1 M acetate buffer solution pH 4.0 and pulse amplitude of 125 mV. (b) Analytical curve. (c) Graph of the collected volume *vs.* filtration time for different diameters. (d) Scanned information on the screen of the cell phone. The error bars indicate the standard deviation of three devices.

Table 1
Results obtained for the determination of pNP in water samples.

Water samples	[pNP] found/µM	Recuperation/%
1*	41.3 (± 1.5)	98.9–106.2
2*	41.5 (± 2.8)	95.5–108.2
3*	38.7 (± 2.5)	91.8–103.8

* The samples were spiked with 40.0 µM pNP.

code to help the analyst perform the analysis, including type of pencil, sample volume, filtration time, analytical curve, concentration levels defined by EPA and more (Fig. 6d). The concentration of pNP in the samples can be obtained in less than 3 minutes using the proposed device combined with the QR code reader of the iPhone. The results of the water sample analysis can be viewed in Table 1. The recovery levels of the three spiked samples varied from 91.8 to 108.2%, indicating that there is no matrix effect observed in the results. It is important to stress that the level of pNP present in the sample was not detected by the device, giving the same signal of the blank.

4. Conclusions

The construction, characterization and application of a three-dimensional electrochemical paper-based analytical device for p-nitrophenol determination in water samples was reported. We demonstrated that low-cost conventional printing paper is an alternative platform for the fabrication of reference and counter electrodes using a drawing process. The carbon tracks formed by soft pencil were characterized by SEM and were free of cracks and wrinkles. The device was characterized by cyclic voltammetry and showed ΔEp of 96 mV, Ipa/Ipc ~1.0 and reversible electrochemical responses for the redox probe studied here ($Fe(CN)_6^{4-/3-}$). For the analytical application, p-nitrophenol was selected as a target molecule and the ePAD gave a detection limit of 1.1 µM for this compound. The proposed 3D layout allows a pump-free filtration, electrochemical detection and proper analysis and interpretation of the result in less than 3 minutes. We believe that 3D layouts for electrochemical paper-based analytical devices will be used in many analytical applications since the folding step is very simple and open many possibilities that may be explored with different detection methods.

Acknowledgements

The authors thank financial support from São Paulo State Research Foundation (FAPESP), Conselho Nacional de Desenvolvimento Científico e Tecnológico (CNPq) and National Institute of Science and Technology in Bioanalytics (INCTBio). MS is indebted to FAPESP for the fellowship. This work was also supported by the Center for Disease Control through the National Institute for Occupational Safety and Health (NIOSH) through grant number OH010050.

Appendix A. Supplementary data

Supplementary data associated with this article can be found, in the online version, at http://dx.doi.org/10.1016/j.electacta.2014.03.109.

References

[1] M.W. Aktar, D. Sengupta, A. Chowdhury, Impact of pesticides use in agriculture: their benefits and hazards, Interdisc. Toxicol. 2 (2009) 1.

[2] S.E. Manahan, Fundamentals of environmental chemistry, CRC press, Boca Raton, 2000.
[3] D.M. Whitacre, Reviews of environmental contamination and toxicology, Springer, New York, 2010.
[4] R.P. Pohanish, Sittig's handbook of toxic and hazardous chemicals and carcinogens, Willian Andrew Inc, Oxford, 2008.
[5] A. Mehdinia, T.B. Kayyal, A. Jabbari, M.O. Aziz-Zanjani, E. Ziaei, Magnetic molecularly imprinted nanoparticles based on grafting polymerization for selective detection of 4-nitrophenol in aqueous samples, J. Chromatogr. A 1283 (2013) 82.
[6] S. Paliwal, M. Wales, T. Good, J. Grimsley, J. Wild, A. Simonian, Fluorescence-based sensing of p-nitrophenol and p-nitrophenyl substituent organophosphates, Anal. Chim. Acta 596 (2007) 9.
[7] H. Zhang, M. Wang, J. Zhao, Z. Shi, Sandwich-type spontaneous injection of nitrophenols for capillary electrophoresis analysis, Anal. Methods 4 (2012) 2177.
[8] A.C. Roy, V.S. Nisha, C. Dhand, M.A. Ali, B.D. Malhotra, Molecularly imprinted polyaniline-polyvinyl sulphonic acid composite based sensor for para-nitrophenol detection, Anal. Chim. Acta 777 (2013) 63.
[9] A.W. Martinez, S.T. Phillips, E. Carrilho, S.W. Thomas III, H. Sindi, G.M. Whitesides, Simple telemedicine for developing regions: camera phones and paper-based microfluidic devices for real-time, off-site diagnosis, Anal. Chem. 80 (2008) 3699.
[10] J. Yan, M. Yan, L. Ge, J. Yu, S. Ge, J. Huang, A microfluidic origami electrochemiluminescence aptamer-device based on a porous Au-paper electrode and a phenyleneethynylene derivative, Chem. Commun. 49 (2013) 1383.
[11] R. Pelton, Bioactive paper provides a low-cost platform for diagnostics, Trends Anal. Chem. 28 (2009) 925.
[12] A.W. Martinez, S.T. Phillips, M.J. Butte, G.M. Whitesides, Patterned paper as a platform for inexpensive, low-volume, portable bioassays, Angew, Chem. Int. Ed. 46 (2007) 1318.
[13] X. Li, D.R. Ballerini, W. Shen, A perspective on paper-based microfluidics: Current status and future trends, Biomicrofluidics 6 (2012) 011301–11311.
[14] W. Dungchai, O. Chailapakul, C.S. Henry, A low-cost, simple, and rapid fabrication method for paper-based microfluidics using wax screen-printing, Analyst 136 (2011) 77.
[15] T. Songjaroena, W. Dungchai, O. Chailapakul, W. Laiwattanapaisal, Novel, simple and low-cost alternative method for fabrication of paper-based microfluidics by wax dipping, Talanta 85 (2011) 2587.
[16] E.W. Nery, L.T. Kubota, Sensing approaches on paper-based devices: a review, Anal. Bioanal. Chem. 405 (2013) 7573.
[17] M. Santhiago, J.B. Wydallis, L.T. Kubota, C.S. Henry, Construction and electrochemical characterization of microelectrodes for improved sensitivity in paper-based analytical devices, Anal. Chem. 85 (2013) 5233.
[18] W. Dungchai, O. Chailapakul, C.S. Henry, Electrochemical Detection for Paper-Based Microfluidics, Anal. Chem. 81 (2009) 5821.
[19] R.F. Carvalhal, M.S. Kfouri, M.H.O. Piazetta, A.L. Gobbi, L.T. Kubota, Electrochemical detection for paper-based separation devices, Anal. Chem. 82 (2010) 1162.
[20] L.Y. Shiroma, M. Santhiago, A.L. Gobbi, L.T. Kubota, Separation and electrochemical detection of paracetamol and 4-aminophenol in a paper-based microfluidic device, Anal. Chim. Acta 725 (2012) 44.
[21] A. Russo, B.Y. Ahn, J.J. Adams, E.B. Duoss, J.T. Bernhard, J.A. Lewis, Pen-on-paper flexible electronics, Adv. Mater. 23 (2011) 3426.
[22] Z. Nie, C.A. Nijhuis, J. Gong, X. Chen, A. Kumachev, A.W. Martinez, M. Narovlyansky, G.M. Whitesides, Electrochemical sensing in paper-based microfluidic devices, Lab Chip 10 (2010) 477.
[23] R.L. McCreery, Advanced carbon electrode materials for molecular electrochemistry, Chem. Rev. 108 (2008) 2646.
[24] Y. Wang, D. Zang, S. Ge, L. Ge, J. Yu, M. Yan, A novel microfluidic origami photoelectrochemical sensor based on CdTe quantum dots modified molecularly imprinted polymer and its highly selective detection of S-fenvalerate, Electrochim. Acta 107 (2013) 147.
[25] J. Lu, S. Ge, L. Ge, M. Yan, J. Yu, Electrochemical DNA sensor based on three-dimensional folding paper device for specific and sensitive point-of-care testing, Electrochim. Acta 80 (2012) 334.
[26] Y. Zhang, L. Ge, S. Ge, M. Yan, J. Yan, D. Zang, J. Lu, J. Yu, X. Song, TiO2–graphene complex nanopaper for paper-based label-free photoelectrochemical immunoassay, Electrochim. Acta 112 (2013) 620.
[27] N. Kurra, G.U. Kulkarni, Pencil-on-paper: electronic devices, Lab Chip 13 (2013) 2866.
[28] N. Dossi, R. Toniolo, A. Pizzariello, F. Impellizzieri, E. Piccin, G. Bontempelli, Pencil-drawn paper supported electrodes as simple electrochemical detectors for paper-based fluidic devices, Electropheresis 34 (2013) 2085.
[29] N. Dosse, R. Toniolo, E. Piccin, S. Susmel, A. Pizzariello, G. Bontempelli, Pencil-drawn dual electrode detectors to discriminate between analytes comigrating on paper-based fluidic devices but undergoing electrochemical processes with different reversibility, Electroanal. 25 (2013) 2515.
[30] P.H.P.C. Tavares, P.J.S. Barbeira, Influence of pencil lead hardness on voltammetric response of graphite reinforcement carbon electrodes, J. Appl. Electrochem. 38 (2008) 827.
[31] M. Santhiago, L.T. Kubota, A new approach for paper-based analytical devices with electrochemical detection based on graphite pencil electrodes, Sens. Act. B 177 (2013) 224.
[32] J. Waters, QR codes for dummies, John Wiley & Sons Inc, New Jersey, 2012.
[33] M.A. Hubbe, Paper's resistance to wetting - A review of internal sizing chemicals and their effects, BioRes. 2 (2007) 106.
[34] M. Lazerges, V.T. Tal, P. Bigey, D. Scherman, F. Bedioui, Electrochemical DNA-biosensors. Two-electrode setup well adapted for miniaturized devices, Sens. Act. B 182 (2013) 510.
[35] A.J. Bard, L. Faulkner, Electrochemical Methods - Fundamental and Applications, Wiley, New York, 2001.
[36] P. Fanjul-Bolado, D. Hernández-Santos, P.J. Lamas-Ardisana, A. Martín-Pernía, A. Costa-García, Electrochemical characterization of screen-printed and conventional carbon paste electrodes, Electrochim. Acta 53 (2008) 3635.
[37] M. Pontié, G. Thouand, F. Nardi, I. Tapsoba, S. Lherbette, Antipassivating electrochemical process of glassy carbon electrode (GCE) dedicated to the oxidation of nitrophenol compounds, Electroanal. 23 (2011) 1579.
[38] N. Kurra, D. Dutta, G.U. Kulkarni, Field effect transistors and RC filters from pencil-trace on paper, Phys. Chem. Chem. Phys. 15 (2013) 8367.
[39] E.V. Anslyn, D.A. Dougherty, Modern physical organic chemistry, University Science, Mill Valley, 2005.
[40] F. Bănică, Chemical sensors and biosensors: fundamentals and applications, J. Wiley & Sons, West Sussex, 2012.
[41] J. Zhong, Q. Zhong, F. Fan, Y. Zhang, Y. Zhang, S. Wang, B. Hu, Z.L. Wang, J. Zhou, Finger typing driven triboelectric nanogenerator and its use for instantaneously lighting up LEDs, Nano Energy 2 (2013) 491.
[42] http://nepis.epa.gov/(accessed in 12.14.2013).
[43] http://water.epa.gov/(accessed in 12.14.2013).